

COHERENT POPULATION TRAPPING WITH COLD ATOMS

T. Zanon, S. Guérandel, E. De Clercq, N. Dimarcq, A. Clairon

BNM-SYRTE – Observatoire de Paris
61 Avenue de l'Observatoire – 75014 Paris - France

Abstract – Atomic clocks based on CPT are interesting because of the narrow linewidths achievable at very low intensities. The linewidth of a CPT resonance in a sample of cold atoms mainly depends on the optical saturation by two lasers and the different relaxation terms responsible for destroying the hyperfine coherence. We propose a complete analytical solution for the excited population based on the classical Bloch formalism to determine the line shape of the resonance. Finally we present the future development of a cold atoms clock based on CPT linewidth.

Keywords – cold atoms, phase locked lasers, sidebands generation, CPT.

I. INTRODUCTION

For atomic clocks, the CPT (coherent population trapping) or EIT (electromagnetically induced transparency) is a phenomenon which enables to obtain sub-natural linewidths with very small intensities, typically 0.1-10 $\mu\text{W}/\text{cm}^2$. CPT appears in a three level system with two separated ground states optically coupled to a common excited level by two coherent fields. This phenomenon is based on the superposition of eigenstates, usually represented by the coupled state $|C\rangle$ and the uncoupled state $|NC\rangle$ [1]:

$$\begin{aligned} |C\rangle &= \frac{\Omega_1}{\sqrt{\Omega_1^2 + \Omega_2^2}} |1\rangle + \frac{\Omega_2}{\sqrt{\Omega_1^2 + \Omega_2^2}} |2\rangle \\ |NC\rangle &= \frac{\Omega_1}{\sqrt{\Omega_1^2 + \Omega_2^2}} |1\rangle - \frac{\Omega_2}{\sqrt{\Omega_1^2 + \Omega_2^2}} |2\rangle \end{aligned} \quad (1)$$

where Ω_1 and Ω_2 are Rabi frequencies of the fields driving transitions $|1\rangle \rightarrow |3\rangle$ and $|2\rangle \rightarrow |3\rangle$. $|NC\rangle$ represents the dark state in which a fraction of the atoms are pumped by spontaneous emission. The linewidth of the dark resonance is extremely sensitive to laser detuning, different Rabi frequencies and incoherent relaxation terms.

In some experiments [3,4], direct modulation of the laser diode current for generating sidebands is commonly used to create coherent beams and drive the dark resonance. But this technique makes difficult any change of the Rabi frequencies for example to observe the effect of linear light shift with frequency offset.

In section II, to complete the study of dark state as a tool for future experiments, we introduce the possibility to drive the dark state with different Rabi frequencies and equal spontaneous decay rates. In sections III and IV, we present the development of an atomic cold atoms clock based on CPT and the optical bench for phase-locking two lasers.

II. BLOCK FORMALISM FOR THE CPT LINESHAPE

To describe the three level system under bichromatic fields, we use the density matrix equation under RWA approximation and we write populations and coherences following an analysis by [5,6].

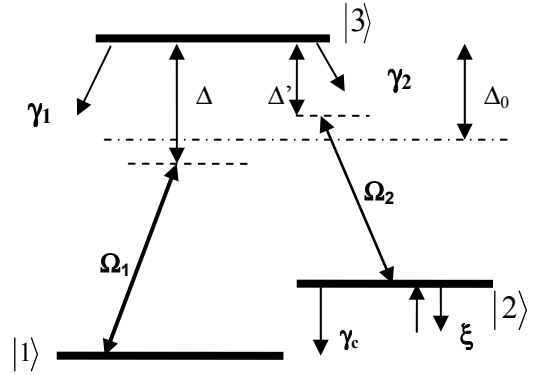


Figure 1: three level diagram for scanning the detuning.

The six equations for the populations σ_{ii} , the two optical coherences σ_{13} and σ_{23} and the hyperfine coherence σ_{12} between the two ground states can be written as [6]:

$$\begin{aligned} \dot{\sigma}_{11} &= 2\Omega_1 \text{Im} \sigma_{13} + \gamma_1 \sigma_{33} + \xi(\sigma_{22} - \sigma_{11}) \\ \dot{\sigma}_{22} &= 2\Omega_2 \text{Im} \sigma_{23} + \gamma_2 \sigma_{33} + \xi(\sigma_{11} - \sigma_{22}) \\ \dot{\sigma}_{33} &= -2\Omega_1 \text{Im} \sigma_{13} - 2\Omega_2 \text{Im} \sigma_{23} - \gamma \sigma_{33} \\ \dot{\sigma}_{12} &= i\Omega_1 \sigma_{32} - i\Omega_2 \sigma_{13} - i[(\Delta - \Delta') - i\gamma_c] \sigma_{12} \\ \dot{\sigma}_{23} &= -i\Omega_1 \sigma_{21} + i\Omega_2 (\sigma_{33} - \sigma_{22}) - i[\Delta' - i\gamma_{c2}] \sigma_{12} \\ \dot{\sigma}_{13} &= i\Omega_1 (\sigma_{33} - \sigma_{11}) - i\Omega_2 \tilde{\sigma}_{12} - i[\Delta - i\gamma_{c1}] \sigma_{12} \end{aligned} \quad (2)$$

with the condition for the hermitian matrix : $\sigma_{ij} = \sigma_{ji}^*$.

$$\text{Im}\{\sigma_{ij}\} = \frac{1}{2i}(\sigma_{ij} - \sigma_{ji}) \text{ and } \text{Re}\{\sigma_{ij}\} = \frac{1}{2}(\sigma_{ij} + \sigma_{ji})$$

We include different damping terms for spontaneous emission called γ_1 and γ_2 . Relaxation terms for the optical coherences are called γ_{c1} and γ_{c2} . Δ_0 is the optical detuning. For each laser frequency, we include the Doppler shift in the detuning :

$$\begin{aligned} \Delta &= \omega_1 - k_1 v - \omega_{13} \\ \Delta' &= \omega_2 - k_2 v - \omega_{23} \end{aligned}$$

The presence of buffer gas or broadening mechanism such as laser linewidths could be taken with additional relaxation constants.

ξ is the relaxation of the difference of populations in the ground state under collisional mechanism.

Finally, we rewrite the detuning as $\Delta = \Delta_0 + \frac{1}{2}(\Delta - \Delta')$ and $\Delta' = \Delta_0 - \frac{1}{2}(\Delta - \Delta')$ like in [6].

1- Generation of sidebands by direct modulation of diode current for $\Omega_1 = \Omega_2$ and $\Omega_1 \neq \Omega_2$.

- **Case $\Omega_1 = \Omega_2$:**

The first case is for equal Rabi frequencies at resonance $\Delta_0=0$ with equal but opposite detuning $\Delta = \delta / 2$ and $\Delta' = -\delta / 2$. We also equal the decay rates $\gamma_1 = \gamma_2 = \gamma$ for spontaneous emission and $\gamma_{e1} = \gamma_{e2} = \gamma / 2$ for optical coherences. We make the assumption that $\delta \ll \gamma$ and $\xi = 0$.

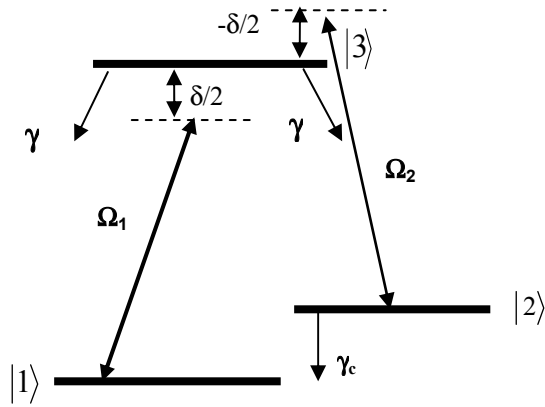


Figure 2: three level diagram for scanning the detuning with sidebands.

Following an analysis by Orriols [6] and Kelley [7], $\Delta w = \sigma_{33} - \sigma_{22}$ and $\Delta n = \sigma_{22} - \sigma_{11}$ are given in appendix and are replaced by their analytical expressions. This leads to a very simple form for the steady state of the excited state:

$$\sigma_{33} = \frac{1}{3}(1 + 2\Delta w + \Delta n) = S \frac{\left(\frac{\delta}{\gamma_c}\right)^2 + \left(1 + 2\frac{\gamma}{\gamma_c}S\right)}{\left(\frac{\delta}{\gamma_c}\right)^2 + \left(1 + 2\frac{\gamma}{\gamma_c}S\right)\left(1 + 3S + 2\frac{\gamma}{\gamma_c}S\right)} \quad (3)$$

with $S = 2 \frac{\Omega^2}{\gamma^2}$ called the optical saturation.

We have for $\delta = 0$ the steady state solution of Orriols [6, eq. (15)] which takes into account the saturation of the transitions under light.

For $\frac{2\gamma}{3\gamma_c} \ll 1$, we have the classical optical saturation:

$$\sigma_{33} = \frac{S}{1 + 3S} \quad (\text{given by Einstein's rates equations}).$$

For $\frac{2\gamma}{3\gamma_c} \gg 1$, the CPT regime starts and we have :

$$\sigma_{33} = \frac{S}{1 + 2\frac{\gamma}{\gamma_c}S}.$$

Finally, we obtain the linewidth :

$$\Delta\nu_{1/2} = 2\gamma_c \sqrt{\left(1 + 2\frac{\gamma}{\gamma_c}S\right)\left(1 + 3S + 2\frac{\gamma}{\gamma_c}S\right)} \quad (4)$$

- **Case $\Omega_1 \neq \Omega_2$:**

The second case is for different Rabi frequencies which complicate a little more the calculation. We finally find after simplifications :

$$\sigma_{33} = S \frac{\left(\frac{\delta}{\gamma_c}\right)^2 + \left(1 + 2\frac{\gamma}{\gamma_c}S^*\right)}{\left(\frac{\delta}{\gamma_c}\right)^2 + \left(1 + 3S + 2\frac{\gamma}{\gamma_c}S^*\right)\left(1 + 2\frac{\gamma}{\gamma_c}S^*\right)} \quad (5)$$

$$\text{with } S = 4 \frac{\Omega_1^2 \Omega_2^2}{\gamma^2 (\Omega_1^2 + \Omega_2^2)} \text{ and } S^* = \frac{\Omega_1^2 + \Omega_2^2}{\gamma^2}$$

The expression of the linewidth becomes :

$$\Delta\nu_{1/2} = 2\gamma_c \sqrt{\left(1 + 2\frac{\gamma}{\gamma_c}S^*\right)\left(1 + 3S + 2\frac{\gamma}{\gamma_c}S^*\right)} \quad (6)$$

For example, unequal Rabi frequencies are present in asymmetric level system as D2 lines in Cs or Rb and are important for studying amplitude and linewidths with an experimental set-up based on phase-locked sources.

We give, in figure 4, the evolution of the resonance drives with (5).

We also recognize the simple expressions given in [4] neglecting the 3S term for the excited population.

To conclude our brief work on the line shape, we can now give the exact solution of the excited population at resonance without approximation.

$$\sigma_{33} = S \frac{\left(\frac{\delta}{\gamma_c}\right)^2 + \left(1 + 2\frac{\gamma}{\gamma_c} S^*\right)}{\left(\frac{\delta}{\gamma_c}\right)^2 \left(1 + \frac{\delta^2}{\gamma^2}\right) + \frac{\delta^2}{\gamma^2} W + \left(1 + 3S + 2\frac{\gamma}{\gamma_c} S^*\right) \left(1 + 2\frac{\gamma}{\gamma_c} S^*\right)} \quad (7)$$

$$\text{with } W = 1 - \frac{4}{\gamma_c^2} \frac{\Omega_1^4 + \Omega_2^4 - \Omega_1^2 \Omega_2^2}{\Omega_1^2 + \Omega_2^2}$$

The lineshape of the resonance is just modified at high detuning and we find that at small detuning the linewidth of the CPT is well fitted again by the formulae (6).

2 – phase-locked lasers for $\Omega_1 \neq \Omega_2$.

We use again the same parameters as above and perform the calculation in the general case directly with different Rabi frequencies and without any approximation..

We compare this case with the technic of scanning the sidebands.

One laser is at resonance $\Delta' = 0$ and the other one is scanned with detuning Δ around the excited state.

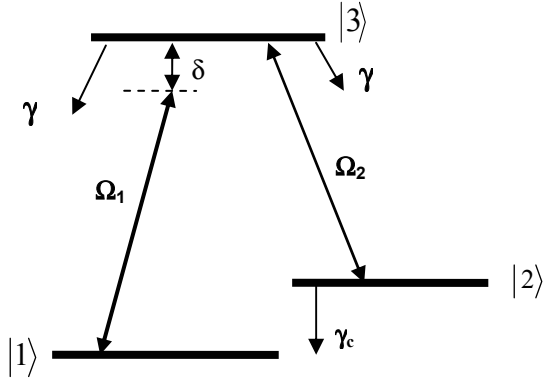


Figure 3: three level diagram for sweeping the detuning with phase- locked device.

We find a similar equation as (7) but with different terms in the detuning behaviour.

$$\sigma_{33} = S \frac{\left(\frac{\delta}{\gamma_c}\right)^2 + \left(1 + 2\frac{\gamma}{\gamma_c} S^*\right)}{\left(\frac{\delta}{\gamma_c}\right)^2 \left(1 + 4\frac{\delta^2}{\gamma^2} \left(\frac{\Omega_2^2}{\Omega_1^2 + \Omega_2^2}\right)\right) + 4\frac{\delta^2}{\gamma^2} W^o + \left(1 + 3S + 2\frac{\gamma}{\gamma_c} S^*\right) \left(1 + 2\frac{\gamma}{\gamma_c} S^*\right)}$$

$$\text{with } W^o = \frac{\Omega_2^2}{\Omega_1^2 + \Omega_2^2} - \frac{1}{\gamma_c^2} \frac{2\Omega_2^4 - \Omega_1^2 \Omega_2^2}{\Omega_1^2 + \Omega_2^2} + \frac{2}{\gamma_c \gamma} \frac{\Omega_1^2 \Omega_2^2}{\Omega_1^2 + \Omega_2^2}$$

We have plotted, in figure 5, formulas (7) and (8) as function of the detuning. We see that for high detuning the wings are quite different in the shape. This can be explained by considering the fact that one of the lasers is always at resonance in the phase locked detuning case and pumping the

excited state although it is not the case for symmetric sweep. At small detuning, the linewidth is well approximated by (6).

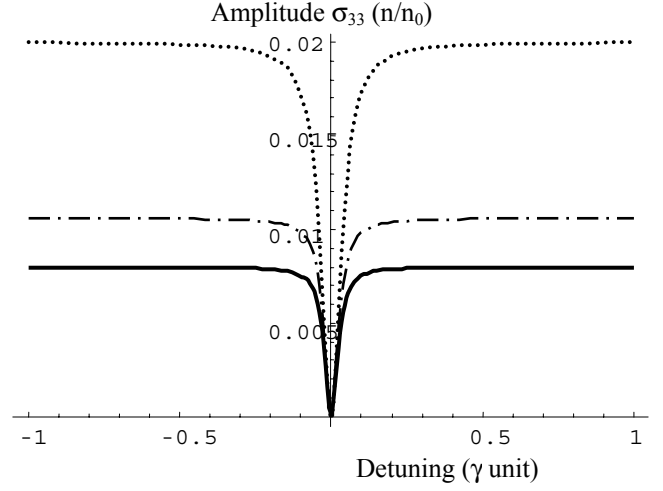


Figure 4:

Resonance for equal Rabi frequencies $\Omega_1 = \Omega_2 = 0.1\gamma$ (dotted curve) with $\gamma = 1$ and $\gamma_c = 0.0001\gamma$. The others cases are $\Omega_1 = 0.1\gamma$, $\Omega_2 = 0.06\gamma$ (dashed) and $\Omega_1 = 0.1\gamma$, $\Omega_2 = 0.05\gamma$ (solid)

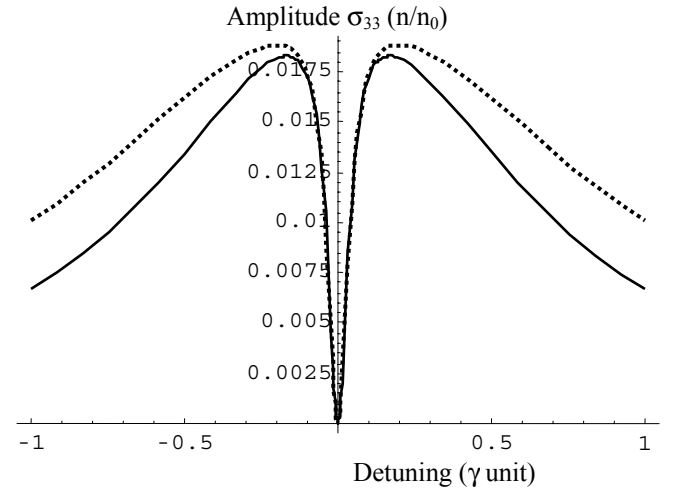


Figure 5:

Lineshapes comparison between sidebands (dotted curve) and the phase-locked method (solid line) for equal Rabi frequencies $\Omega_1 = \Omega_2 = 0.1\gamma$ with $\gamma = 1$ and $\gamma_c = 0.0001\gamma$.

Finally, to check that the complete analytical solution used is correct, we have numerically plotted the steady state solution for the excited population σ_{33} with the integration of Bloch equations. We set as boundary conditions :

$$\begin{aligned}
\sigma_{33}(t=0) &= 0 \\
\sigma_{22}(t=0) &= 1/2 \\
\sigma_{11}(t=0) &= 1/2 \\
\sigma_{12}(t=0) &= \sigma_{23}(t=0) = \sigma_{13}(t=0) = 0
\end{aligned}$$

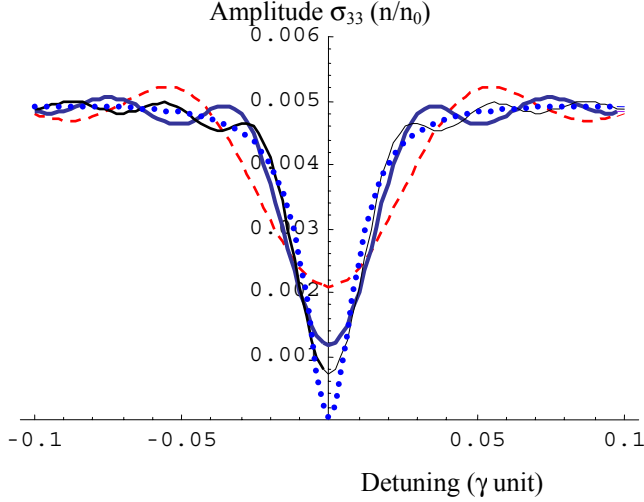


Figure 6 a:

Resonance for $\Omega_1 = \Omega_2 = 0.05\gamma$ and $\gamma_c = 0.0001\gamma$ but at three different times $t_1 = 90/\gamma$ (solid) , $t_2 = 150/\gamma$ (dashed) , $t_3 = 200/\gamma$ (thin curve) . The dotted line is the analytical steady state solution for σ_{33} obtains from (7).

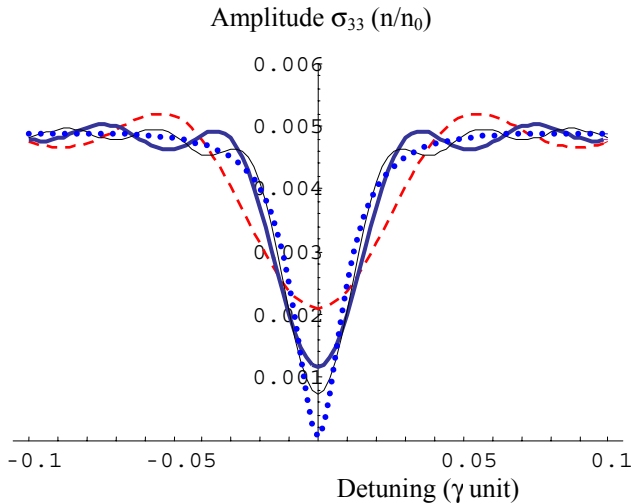


Figure 6 b:

Resonance for $\Omega_1 = \Omega_2 = 0.05\gamma$ and $\gamma_c = 0.0001\gamma$ but at three different times $t_1 = 90/\gamma$ (solid) , $t_2 = 150/\gamma$ (dashed) , $t_3 = 200/\gamma$ (thin curve) . The dotted line is the analytical steady state solution for σ_{33} obtains from (8).

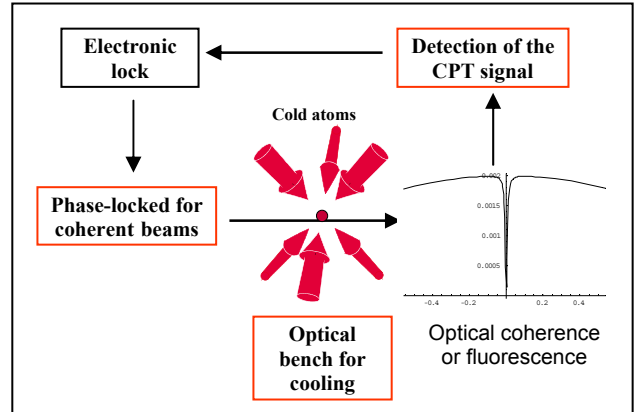
We compare these numerical results with our analytical solutions (7) and (8). As expected, the three numerical curves in each case tend to the analytical steady state limit at infinite time (figure 6a and 6b).

III. DESIGN OF A COLD ATOM CLOCK BASED ON CPT

Usually, two methods of generating the coherent beams are preferred : direct modulation of the current diode and phase-locked lasers. In order to achieve sub-natural linewidth, typically below 100 Hz [2,3], a buffer gas is introduced with the atoms to increase the transit time and quench the fluorescence, to avoid the destruction of the hyperfine coherence (Lamb Dicke regime). Unfortunately, a collisional shift due to the buffer gas is present which degrades the accuracy of the clock.

We propose to develop a new atomic clock based on CPT with cold atoms. Cold atoms cancel the Doppler broadening as the buffer gas but the collisional shift is greatly reduced.

We have made the choice for metrological applications to develop the phase-locked system to study the effect of different Rabi frequencies. It is more difficult with a modulation of the laser to control the amplitudes of the sideband. The phase locked system also allows us to change easily the frequency offset to study the role of the Raman detuning in the light shift.



The time sequence of our future clock will be the same as for atomic fountains without launching the atoms. We prepare the atoms in the ground state with optical pumping and cool them in a classical optical molasses. Then we interrogate the atoms with the coherent beams to generate the superposition of states called the dark state. We have the choice to detect this dark state by the fluorescence (σ_{33}) or detect the optical coherence (σ_{13}) or (σ_{23}) in absorption.

IV. EXPERIMENTAL SET-UP

To drive the dark resonance in cesium, two coherent laser beams with 9.2 GHz frequency offset have to be generated. We want to cool atoms on D2 transitions and make the choice to use D1 transitions to generate the CPT beams. D1 transitions are interesting for many points of view:

- The splitting between two levels in the excited state (1.2 GHz) is larger than the Doppler broadening (380 MHz) which cancel crossover resonances.
 - The Clebsch-Gordan coefficients are symmetric and gives a efficient pumping of atoms in the dark state.
- This lambda system is then very close to a pure three level system as treated above.

A) laser sources at 894 nm

We have developed two ECLD lasers at 894 nm in a littrow configuration. The length of the cavity is 55 mm and the output power is about 10 mW. We achieve 2.7 GHz tuning range without mode hops.

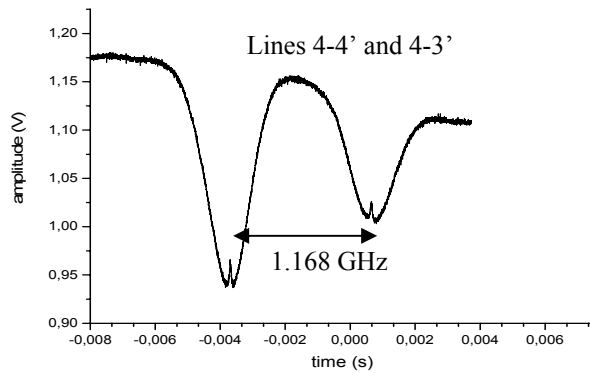
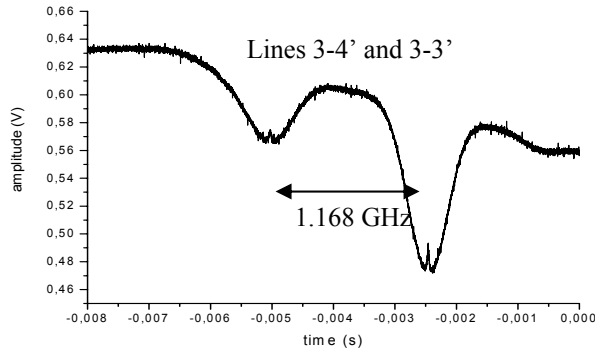


Figure 7a and 7b:

Classical saturated absorption for Cesium at 894 nm. We see the absence of cross-over resonances.

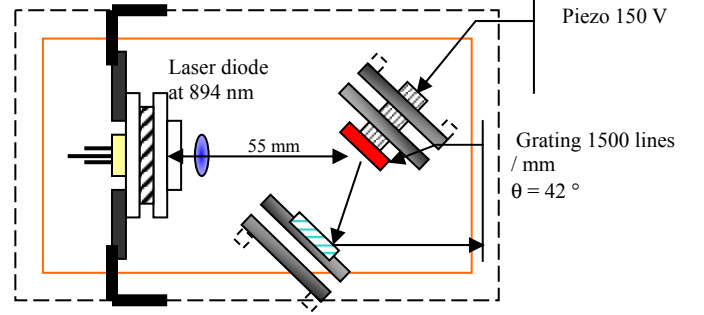
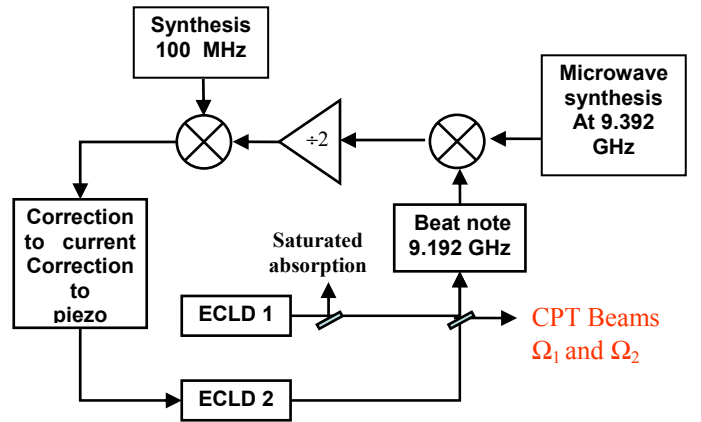


Figure 8: *schematic view of one ECLD.*

B) phase-locked device

The CPT resonant Raman beams are generated by two diodes lasers, which are phase-locked to each other with a 9.2 GHz frequency offset. The reference frequency at 9.392 GHz is summed out with a beat note at 9.192 GHz and a rf digital synthesiser (100 MHz).



The beams from the two lasers are overlapped in a polarizing beam splitter cube and part of this light is sent through a linear polarizer at 45° to a fast photodiode.

The error signal generated by the electronic phase-locked device is used to feed back to one of the lasers. The feed back corrections are separated in two ways. Low frequency are sent to the PZT transducer, and high frequency are added directly to the diode current.

The CPT beams go through an AOM (80 MHz) before being injected in a polarization maintaining fiber that controls their intensity and lets the possibility to switch off the beams to generate CPT pulses. The CPT beams will be sent to the cold atomic cloud for the clock interrogation.

IV. CONCLUSION

We have now established in a pure three level system based on Bloch formalism the exact steady states equations to study the effect of different Rabi frequencies, linear light shift and

spontaneous emission. The possibility to calculate analytical solutions without any approximation is now clearly demonstrated. It is also possible to derive an analytical solution of the linewidth obtained in classical EIT experiments with a Doppler broadened vapor. However, this very simple model does not take into account the multi-Zeeman sublevels in a magnetic field [8].

V. ACKNOWLEDGMENT

Many people have contributed to this work. We think specially Jacques Vanier and Claude Audoin for their helpful discussions. We are thankful to L. Volodimer, M. Lours, M. Dequin and G. Santarelli from the electronic group for their contribution to the phase-locked device.

VI. APPENDIX

Here, we give the two differences of population $\Delta w = \sigma_{33} - \sigma_{22}$ and $\Delta n = \sigma_{22} - \sigma_{11}$ in the particular case of equal but opposite detunings $\Delta = \delta/2$ and $\Delta' = -\delta/2$:

$$\Delta w = -\frac{\Omega_1^2}{\Omega_1^2 + \Omega_2^2} \frac{\left(1 + \frac{\delta}{\gamma_c}\right)^2 \left(1 + \frac{\delta^2}{\gamma^2}\right) + 4 \frac{\Omega_1^2 + \Omega_2^2}{\gamma^2 \gamma_c^2} (-\delta^2 + \gamma_c + \Omega_1^2 + \Omega_2^2)}{\left(\frac{\delta}{\gamma_c}\right)^2 \left(1 + \frac{\delta^2}{\gamma^2}\right) + \frac{\delta^2}{\gamma^2} W + \left(1 + 3S + 2 \frac{\gamma}{\gamma_c} S^*\right) \left(1 + 2 \frac{\gamma}{\gamma_c} S^*\right)}$$

$$\Delta n = \frac{(\Omega_1^2 - \Omega_2^2)}{\Omega_1^2 + \Omega_2^2} \frac{\left(1 + \frac{\delta}{\gamma_c}\right)^2 \left(1 + \frac{\delta^2}{\gamma^2}\right) + 4 \frac{\Omega_1^2 + \Omega_2^2}{\gamma^2 \gamma_c^2} (-\delta^2 + \gamma_c + \Omega_1^2 + \Omega_2^2)}{\left(\frac{\delta}{\gamma_c}\right)^2 \left(1 + \frac{\delta^2}{\gamma^2}\right) + \frac{\delta^2}{\gamma^2} W + \left(1 + 3S + 2 \frac{\gamma}{\gamma_c} S^*\right) \left(1 + 2 \frac{\gamma}{\gamma_c} S^*\right)}$$

$$\text{with } W = 1 - \frac{4}{\gamma_c^2} \frac{\Omega_1^4 + \Omega_2^4 - \Omega_1^2 \Omega_2^2}{\Omega_1^2 + \Omega_2^2}$$

We can see that Δn is zero for equal Rabi frequencies. It means that half of population are dispatched in the ground state levels even if Ω_1 and Ω_2 are small and the superposition of coherent states is still formed.

REFERENCES

- [1] E. Arimondo, "Coherent population trapping in laser spectroscopy", *Prog. Opt. XXXV*, pp. 257, 1996.
- [2] R. Wynands, A. Nagel, "Precision spectroscopy with coherent dark states", *Applied Physics B*, vol. 68, pp. 1-25, 1999.
- [3] M. Merimaa, T. Lindvall, I. Tittonen, E. Ikonen, "All-optical atomic clocks based on coherent population trapping in ^{85}Rb ", *J. Optics. Soc. Am. B*, vol. 20, No 2, pp.273-279, February 2003.
- [4] J. Vanier, A. Godone and F. levi, "Coherent population trapping in Cesium : Dark lines and coherent microwave emission.", *Physical review A*, vol. 58, pp. 2345-25, September 1998.
- [5] R. Brewer, E.L. Hahn, "Coherent two-photon processes: Transient and steady state cases", *Physical review A*, vol. 11, pp. 1641-1649, May 1975.
- [6] G. Orriols, "Nonabsorption resonances by nonlinear coherent effects in a three level system", *Il Nuovo Cimento, B* 53 vol. 1, No 1, pp. 1-23, September 1979.
- [7] P. L. Kelley, P. J. Harshman, O. Blum, T.K. Gustafson, "radiative renormalisation analysis of optical double resonance", *J. Optics. Soc. Am. B*, vol. 11, No 11, pp.2298-2302, November 1994.
- [8] A.V. Taichenachev, V.I. Yudin, R. Wynands, M. Stähler, J. Kitching, L. Hollberg, "Theory of dark resonances for alkali-metal vapors in a buffer gas cell", *Physical review A*, vol. 67, 033810-1, pp. 1-11, March 2003.